Tripling of the Unit Cell Volume of the Non-centrosymmetric $AlPO_4$-SOD after Dehydration: A Structural Study of a Reversible Process

Jean-Louis Paillaud,*,† Claire Marichal,† Mélanie Roux,† Christian Baerlocher,‡ and Jean Michel Chézeau†

Laboratoire de Matériaux à Porosité Contrôlée, UMR 7016, ENSCMu, Université de Haute Alsace, 3 rue Alfred Werner, 68093 Mulhouse Cedex, France, and Laboratorium für Kristallographie, Wolfgang-Pauli-Strasse 10, ETH-Hönggerberg, HCI G 507 CH-8093 Zürich, Switzerland

Received: February 12, 2005; In Final Form: April 25, 2005

The structure of $AlPO_4$-**SOD**, a microporous aluminophosphate synthesized in a quasi-nonaqueous system using dimethylformamide as template and solvent, was previously reported. Then, various solid state nuclear magnetic resonance techniques applied on the dehydrated compound at 200 °C were performed and suggested a rearrangement of one-third of the template molecules inside the sodalite cages and a tripling of the unit cell parameter *c*. We present here the structure determined from molecular modeling and Rietveld analysis on synchrotron data of $AlPO_4$-**SOD** dehydrated under vacuum at 100 °C together with some solid state NMR experiments of the rehydrated product.

1. Introduction

The synthesis of novel crystalline microporous aluminophosphate molecular sieves ($AlPO_4$-*n*), pioneered by Wilson et al.,[1] has been extremely successful, since it led to numerous framework topologies, among which several are still unknown in the aluminosilicate family.[2] The main reason for such a diversity has to be seen in the ability for the aluminum species in these materials to be 4-, 5-, or 6-fold coordinated. Unfortunately, the potential applications of these materials and their partly substituted derivatives as catalysts are limited by the high sensitivity of their emptied framework to water. Indeed, the framework aluminums are able to modify their coordination by bonding to water molecules.[3−6] Consequently, studies to understand the hydration and dehydration mechanisms of AlPO's are of tremendous interest.

An aluminophosphate material which was first synthesized by Vidal et al.[7] from a quasi-nonaqueous medium using dimethylformamide (DMF) as both solvent and template has been given the name $AlPO_4$-**SOD** because its framework exhibits the stacking of β-cages characteristic of the **SOD** framework type. However, these cages are strongly distorted, due to 6-fold coordinated aluminums bonded to both the carbonyl oxygen of a DMF molecule and the oxygen of a water molecule. The symmetry of the unit cell is lowered to monoclinic, compared to the cubic symmetry of $AlPO_4$-20 of the same framework topology obtained under hydrothermal conditions with the tetramethylammonium ion as a template.[8]

The simultaneous presence of an organic template and a water molecule is not unique in the $AlPO_4$ family, but Vidal et al. have shown that, in $AlPO_4$-**SOD**, water molecules are eliminated at 170 °C, whereas the material has to be calcined above 400 °C in order to remove the DMF. This results in the existence of an intermediate dehydrated phase which still hosts the DMF. Such an intermediate phase does not seem to have been studied in other $AlPO_4$'s which contain both water and a template probably because, in most cases, they are removed in overlapping temperature ranges.

In a previous paper,[9] the as-synthesized, dehydrated, and calcined $AlPO_4$-**SOD** materials were investigated by various solid state NMR and powder X-ray diffraction techniques. A structure refinement from powder synchrotron data and a complete assignment of ^{31}P and ^{27}Al resonances to the corresponding crystallographic sites of the as-synthesized material was achieved. To explain the modification of the ^{27}Al MAS NMR spectra upon dehydration, a structural rearrangement of the DMF template molecules was proposed. The structure of the material calcined at 800 °C was solved from powder X-ray diffraction data and found in agreement with the NMR spectra. The aim of the present study is (a) to further support the rearrangement mechanism by locating the DMF in the dehydrated phase and (b) to investigate the reversibility of the dehydration/rehydration cycle, which in that case should revert to the as-synthesized material, a case which cannot be observed in the materials where the template removal overlaps that of the removed water molecules.

2. Experimental Section

2.1. Sample Preparation. The aluminophosphate $AlPO_4$-**SOD** was synthesized according to Vidal et al.,[7] using dimethylformamide (DMF) as template and solvent, and is the same as the one used in the previous study.[9] Briefly, gels with a molar composition of $1.0Al_2O_3$:$1.0P_2O_5$:$3.5H_2O$:7.8DMF were heated in a Teflon lined autoclave at 130 °C for 7 days. The resulting crystalline product was filtered, washed with distilled water, and dried at 80 °C overnight. Dehydration of the sample was performed by heating the as-synthesized material in a dry air flow at a rate of 1 °C·min^{-1} to 200 °C with a plateau of 12 h at this temperature. The NMR rotors were filled in an argon atmosphere of a glovebox. ^1H solid state NMR results on the dehydrated material confirm the total elimination of the water molecules. For the X-ray analyses of the rehydrated samples,

* Corresponding author. Fax: (+33) 3 89 33 68 85. E-mail: Jean-Louis.PAILLAUD@uha.fr.
† Université de Haute Alsace.
‡ ETH.

10.1021/jp050763e CCC: $30.25
Published on Web 05/26/2005

TABLE 1: Crystallographic Parameters of Dehydrated $AlPO_4$-SOD[a]

synchroton data collection at ESRF, Grenoble, Swiss-Norwegian beamline BM1-B	
wavelength (Å)	0.79965(1)
Rietveld refinement program	GSAS[12] with EXPGUI interface[12]
chemical formula	$\|(CH_3)_2NCHO\|$ $[Al_3P_3O_{12}]$
calculated molecular formula weight (g)	438.95
space group	*Cc* (no. 8)
a (Å)	12.8203(1)
b (Å)	12.1827(1)
c (Å)	26.9924(2)
β (°)	91.84(0)
V (Å^3)	4213.64(6)
Z	12
density (calculated) (g.cm^{-3})	2.076
number of observation	8694
number of contributing reflections	2936
number of structural parameters	275
number of profile parameters	16
[b] $R_p = \Sigma\{[\|y_o - y_c\| \times \|y_o - y_b\|/y_o]/\Sigma \|y_o - y_b\|\}$	0.0328
[b] $wR_p = \{\Sigma[w \times (y_o - y_c) \times (y_o - y_b)/y_o]^2/\Sigma[w \times (y_o - y_b)^2]\}^{1/2}$	0.0441
[c] wR_{exp}	0.0147
[c] R_F	0.0264
[c] R_F^2	0.0366
[c] χ^2	8.775
largest diff peak and hole (e·Å^{-3})	0.264, −0.212

[a] After the Rietveld refinement, the phase fractions (%) are 93.38(8) and 6.62(8) for $AlPO_4$-**SOD** and $AlPO_4$-**GIS**, respectively. [b] y_o, y_c, and y_b are *y* observed, *y* calculated, and *y* background, respectively. [c] The definitions of these residual values are given in ref 12.

identical thermal treatment was performed in capillaries placed in the oven. The rehydrated samples were obtained at ambient temperature by exposure to moisture over a saturated aqueous solution of NH_4Cl (constant humidity 0.80) for various periods of time (48 h, 43 days, and 1 year).

2.2. X-ray Diffraction. *2.2.1. Dehydrated $AlPO_4$-SOD*. The high-resolution powder X-ray diffraction data were collected at the European Synchrotron Radiation Facility (ESRF, Grenoble) on the Swiss-Norwegian line BM1-B. The $AlPO_4$-**SOD** was dehydrated under vacuum at 100 °C for 48 h and then filled into a capillary (Ø = 1 mm) under dry air and sealed. After dehydration, the sample contains a small amount of $AlPO_4$-**GIS**[10] of topology **GIS**[2] as an impurity. Structure analysis was performed using the molecular modeling program Cerius2[11] from the earlier published crystallographic data of the as-synthesized $AlPO_4$-**SOD**,[9] and the Rietveld refinement was performed using the GSAS package[12] using the synchrotron data. In Cerius2, a super unit cell was generated by tripling the unit cell parameter *c* of as-synthesized $AlPO_4$-**SOD** in space group *P*1. Next, the parameters *a*, *b*, *c*, and β were changed to the values obtained by indexing of the powder pattern. Each of the three DMF molecules was kept attached to one aluminum atom via the carbonyl oxygen atom, but the water molecules were removed. Then, the structure was relaxed from energy minimization, while the unit cell parameters were fixed. When the minimum of energy was reached, the space group was changed to *Cc*, as earlier suggested.[9] At this stage, the asymmetric unit of the model contained nine aluminum atoms of which three were pentacoordinated to four framework oxygen atoms and one carbonyl oxygen of the DMF molecule. As deduced from the previously published solid state NMR study and following the dehydration mechanism proposed at that time,[9] one molecule of DMF was moved from one Al site to a neighboring pentacoordinated Al site, thus forming one hexacoordinated aluminum $Al(DMF)_2O_4$ species.

After a new cycle of minimization, the previous proposed model was introduced in GSAS for the Rietveld refinement. All the atoms were refined isotropically. Soft constraints were placed on the bond lengths and angles of the framework, and adequate sets of constraints were defined to transform the three crystallographic distinct DMF molecules to almost-rigid bodies including the hydrogen atoms. Several cycles of refinement and Fourier difference map calculations were required before the true position of the hexacoordinated ($Al(DMF)_2O_4$) aluminum could be found.

During the Rietveld refinement, it was not essential to refine the crystal structure of the $AlPO_4$-**GIS** impurity. It was sufficient to refine the unit cell parameters (S.G. $P2_1/c$) which changed slightly from $a = 9.412(3)$ Å, $b = 12.770(4)$ Å, $c = 8.594(3)$ Å, and $\beta = 112.84(6)°$ for the fluorinated material[10] to $a = 9.405(1)$ Å, $b = 12.774(1)$ Å, $c = 8.581(1)$ Å, and $\beta = 112.80(1)°$ in the present study. This was possible because both structures are probably isostructural and F^- and OH^- have the same scattering power (see discussion below). In any case, the small amount of this material would probably not have allowed a proper Rietveld refinement. Successful convergence was obtained with $R_p = 0.0328$, $wR_p = 0.0441$, $R_F = 0.0264$, and $\chi^2 = 8.775$. The Rietveld refinement led to a [$AlPO_4$-**SOD**]/[$AlPO_4$-**GIS**] molar ratio of about 14.1. Further details of the crystallographic data are given in Table 1. The final atomic parameters are given in Table 2 and Supporting Information Table 1S. In Table 3 and Supporting Information Tables 2S and 3S, bond distances and selected bond angles are reported, respectively. The final plot of the Rietveld refinement is given in Figure 1.

2.2.2. Rehydrated Samples. The dehydrated sample used for the rehydration study did not contain any traces of $AlPO_4$-**GIS**. The data collection for the rehydrated samples was performed at room temperature using a STOE STADI-P diffractometer in the Debye−Scherrer geometry, equipped with a linear position-sensitive detector (6° in 2θ) and using Ge monochromated Cu Kα_1 radiation ($\lambda = 1.5406$ Å).

2.3. NMR Measurements. The ^{1}H, ^{31}P, and ^{27}Al NMR experiments were performed on a Bruker DSX-400 spectrometer ($B_0 = 9.4$ T) at $\nu_0 = 400.1$, 161.9, and 104.2 MHz, respectively. For the dehydrated/rehydrated samples, ^{1}H MAS NMR experiments were performed with a 2.5 mm Bruker MAS probe with spinning frequencies ranging from 10 to 25 kHz, a $\pi/2$ pulse duration of 3 μs, and a recycle delay of 6 s. ^{31}P and ^{27}Al magic angle spinning (MAS) NMR experiments were recorded on a

TABLE 2: Atomic Parameters, Isotropic Displacement Parameters (U_i), and Occupancy Parameters of Dehydrated $AlPO_4$-SOD[a]

atom	Wyck	*x*	*y*	*Z*	*U* (Å^2)
P1	4*a*	0.3769(6)	0.6123(7)	0.19984(31)	0.0235(4)[b]
P2	4*a*	0.1161(7)	0.3822(7)	0.21066(31)	0.0235(4)[b]
P3	4*a*	0.2413(8)	−0.0165(5)	0.2911(4)	0.0235(4)[b]
P4	4*a*	0.3639(6)	0.3700(6)	0.04015(32)	0.0235(4)[b]
P5	4*a*	0.1239(6)	0.6301(6)	0.04148(32)	0.0235(4)[b]
P6	4*a*	0.2463(7)	1.0194(6)	0.12496(33)	0.0235(4)[b]
P7	4*a*	0.3656(6)	0.3838(7)	0.36788(30)	0.0235(4)[b]
P8	4*a*	0.0938(6)	0.6097(7)	0.38284(31)	0.0235(4)[b]
P9	4*a*	0.2234(7)	1.0127(6)	0.45552(32)	0.0235(4)[b]
Al1	4*a*	0.2357(8)	0.4820(7)	0.1227(4)	0.0320(6)[c]
Al2	4*a*	0.3700(7)	0.8738(7)	0.20555(35)	0.0320(6)[c]
Al3	4*a*	0.1215(7)	0.1239(8)	0.21026(35)	0.0320(6)[c]
Al4	4*a*	0.2350(9)	0.5450(6)	0.2898(5)	0.0320(6)[c]
Al5	4*a*	0.3751(7)	0.1009(8)	0.0355(4)	0.0320(6)[c]
Al6	4*a*	0.1098(7)	0.8863(7)	0.0463(4)	0.0320(6)[c]
Al7	4*a*	0.2480(8)	0.4880(7)	0.4579(4)	0.0320(6)[c]
Al8	4*a*	0.3574(7)	0.1228(8)	0.37725(33)	0.0320(6)[c]
Al9	4*a*	0.1036(7)	0.8722(7)	0.37062(33)	0.0320(6)[c]
O1	4*a*	0.1669(11)	0.0443(11)	0.2592(5)	0.0262(4)[d]
O2	4*a*	0.1367(12)	0.2634(10)	0.2242(5)	0.0262(4)[d]
O3	4*a*	−0.0074(9)	0.0974(11)	0.1975(6)	0.0262(4)[d]
O4	4*a*	0.2981(11)	0.3940(12)	0.0837(5)	0.0262(4)[d]
O5	4*a*	0.1589(12)	0.4508(11)	0.2534(5)	0.0262(4)[d]
O6	4*a*	0.3037(11)	0.9342(12)	0.1560(5)	0.0262(4)[d]
O7	4*a*	0.3270(11)	0.5603(12)	0.1535(5)	0.0262(4)[d]
O8	4*a*	0.3247(11)	0.9240(12)	0.2621(5)	0.0262(4)[d]
O9	4*a*	0.3525(12)	0.7356(10)	0.1996(6)	0.0262(4)[d]
O10	4*a*	−0.0006(9)	0.4008(12)	0.2017(6)	0.0262(4)[d]
O11	4*a*	0.1702(11)	0.4058(12)	0.1637(5)	0.0262(4)[d]
O12	4*a*	0.1518(11)	0.9244(12)	−0.0114(5)	0.0262(4)[d]
O13	4*a*	0.1699(11)	0.9630(11)	0.0915(5)	0.0262(4)[d]
O14	4*a*	0.1435(11)	0.7490(10)	0.0551(6)	0.0262(4)[d]
O15	4*a*	−0.0252(9)	0.9023(12)	0.0514(6)	0.0262(4)[d]
O16	4*a*	0.3378(11)	0.5548(13)	0.2460(5)	0.0262(4)[d]
O17	4*a*	0.1498(11)	0.5591(12)	0.0882(5)	0.0262(4)[d]
O18	4*a*	0.2941(11)	0.0677(12)	−0.0165(5)	0.0262(4)[d]
O19	4*a*	0.3263(11)	0.4342(12)	−0.0063(5)	0.0262(4)[d]
O20	4*a*	0.3240(11)	0.0843(13)	0.0963(5)	0.0262(4)[d]
O21	4*a*	0.3504(12)	0.2499(10)	0.0276(6)	0.0262(4)[d]
O22	4*a*	0.0089(9)	0.6171(12)	0.0285(6)	0.0262(4)[d]
O23	4*a*	0.1901(11)	0.6027(12)	−0.0024(5)	0.0262(4)[d]
O24	4*a*	0.1901(11)	0.0968(12)	0.1586(5)	0.0262(4)[d]
O25	4*a*	0.3327(11)	0.4236(12)	0.4186(5)	0.0262(4)[d]
O26	4*a*	0.1788(11)	0.9003(11)	0.3202(5)	0.0262(4)[d]
O27	4*a*	0.1539(11)	0.9438(12)	0.4225(5)	0.0262(4)[d]
O28	4*a*	0.1050(11)	0.7340(9)	0.3834(5)	0.0262(4)[d]
O29	4*a*	−0.0201(9)	0.9143(11)	0.3590(5)	0.0262(4)[d]
O30	4*a*	0.1568(11)	0.5641(12)	0.4262(5)	0.0262(4)[d]
O31	4*a*	0.2980(11)	0.0640(11)	0.3251(5)	0.0262(4)[d]
O32	4*a*	0.2941(12)	0.4261(11)	0.3247(5)	0.0262(4)[d]
O33	4*a*	0.2858(11)	0.0924(11)	0.4255(5)	0.0262(4)[d]
O34	4*a*	0.3629(11)	0.261(1)	0.3699(5)	0.0262(4)[d]
O35	4*a*	−0.0188(9)	0.5808(12)	0.3895(6)	0.0262(4)[d]
O36	4*a*	0.1298(12)	0.5551(14)	0.3342(5)	0.0262(4)[d]

[a] Standard deviations are given in parentheses. [b−d] These parameters were constrained to be equal.

TABLE 3: Selected Interatomic Distances (Å) of Dehydrated $AlPO_4$-SOD[a,b]

P1−O3^{vii}	1.498(14)	Al1−O11	1.689(17)
P1−O7	1.524(16)	Al1−O17	1.702(17)
P1−O9	1.534(15)	Al2−O6	1.726(16)
P1−O16	1.528(17)	Al2−O8	1.760(17)
P2−O2	1.514(15)	Al2−O9	1.705(15)
P2−O5	1.513(16)	Al2−O10^{vii}	1.698(15)
P2−O10	1.525(15)	Al3−O1	1.725(16)
P2−O11	1.492(16)	Al3−O2	1.750(16)
P3−O1	1.465(17)	Al3−O3	1.708(15)
P3−O8^{i}	1.528(17)	Al3−O24	1.705(17)
P3−O26^{i}	1.525(16)	Al4−O5	1.781(17)
P3−O31	1.513(16)	Al4−O16	1.803(19)
P4−O4	1.498(16)	Al4−O32	1.875(17)
P4−O15^{viii}	1.497(14)	Al4−O36	1.837(19)
P4−O19	1.542(16)	Al4−O1′	1.946(17)
P4−O21	1.511(14)	Al4−O2′	1.905(17)
P5−O14	1.513(15)	Al5−O18	1.766(17)
P5−O17	1.556(16)	Al5−O20	1.798(17)
P5−O22	1.513(14)	Al5−O21	1.854(16)
P5−O23	1.516(16)	Al5−O22^{viii}	1.743(15)
P6−O6	1.510(16)	Al5−O3′	1.920(15)
P6−O13	1.480(16)	Al6−O12	1.728(17)
P6−O20^{ii}	1.505(17)	Al6−O13	1.701(17)
P6−O24^{iii}	1.508(17)	Al6−O14	1.742(15)
P7−O25	1.525(16)	Al6−O15	1.751(15)
P7−O29^{viii}	1.538(14)	Al7−O19^{iv}	1.667(17)
P7−O32	1.548(16)	Al7−O23^{iv}	1.724(17)
P7−O34	1.497(15)	Al7−O25	1.730(17)
P8−O28	1.521(14)	Al7−O30	1.701(17)
P8−O30	1.507(16)	Al8−O31	1.734(16)
P8−O35	1.502(14)	Al8−O33	1.659(17)
P8−O36	1.555(17)	Al8−O34	1.697(16)
P9−O12^{iii}	1.510(17)	Al8−O35^{viii}	1.690(15)
P9−O18^{iv}	1.519(16)	Al9−O26	1.727(17)
P9−O27	1.497(16)	Al9−O27	1.755(16)
P9−O33^{ii}	1.510(16)	Al9−O28	1.719(14)
Al1−O4	1.718(17)	Al9−O29	1.687(15)
Al1−O7	1.705(17)		

[a] Standard deviations are given in parentheses. [b] Symmetry codes: (i) *x*, −1 + y, *z*; (ii) *x*, 1 + *y*, *z*; (iii) *x*, 2 − *y*, 0.5 + *z*; (iv) *x*, 1 − *y*, 0.5 + *z*; (v) *x*, 2 − *y*, −0.5 + *z*; (vi) *x*, 1 − *y*, −0.5 + *z*; (vii) 0.5 + *x*, 0.5 + *y*, *z*; (viii) 0.5 + *x*, −0.5 + *y*.

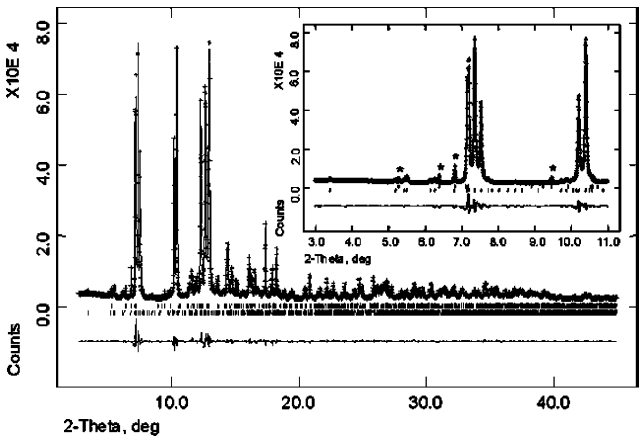

Figure 1. Rietveld refinement of dehydrated $AlPO_4$-**SOD**: experimental (crosses); calculated (full line); difference plot (bottom line). The short vertical lines mark the positions of possible Bragg reflections: top, $AlPO_4$-**GIS**; bottom, dehydrated $AlPO_4$-**SOD**. The inset gives the low angle region where stars indicate the position of the main reflections of the $AlPO_4$-**GIS** impurity.

standard double bearing probe with a 4 mm diameter ZrO_2 rotor, with spinning frequencies ranging from 3.5 to 10 kHz. ^{31}P MAS NMR spectra were acquired with a $\pi/2$ pulse duration of 3.5 μs, and a recycle time of 193 s must be used in order to avoid saturation. The ^{27}Al MAS NMR spectra were recorded with a short recycle time of 0.5 s and by using a 0.8 μs single pulse excitation, corresponding to a flip angle of $\pi/12$ in order to ensure selective excitation of the central transition. The *Z*-filter version of the MQMAS sequence[13] was used to acquire the ^{27}Al 3QMAS spectrum. The triple quantum coherence was excited with a radio frequency field strength of 227 kHz, corresponding to pulse durations of 3 μs and 1 μs for the first two pulses. For converting the zero quantum into single-quantum coherence, the last pulse ($\pi/2$ selective) was adjusted to 10 μs. The 3QMAS experiment was performed with a 2.5 mm Bruker probe at a spinning frequency of 15 kHz. Simulations of quadrupolar line shapes to estimate the quadrupolar coupling constant (C_Q) and

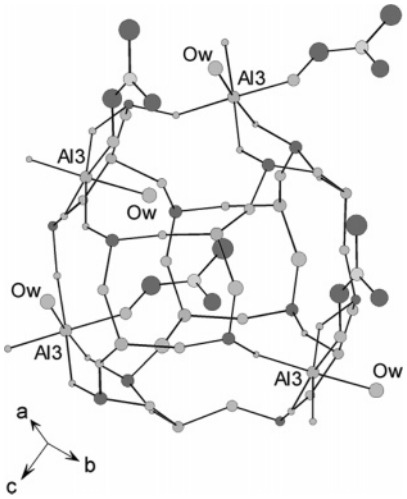

Figure 2. View of one sodalite cage of as-synthesized $AlPO_4$-**SOD** in which four equivalent Al3 are 6-fold coordinated ($Al(DMF)(H_2O)O_4$).

the asymmetry parameter (η_Q) of each Al site were realized with the WINFIT software.[14] ^1H, ^{31}P, and ^{27}Al chemical shifts are relative to TMS, H_3PO_4 (85 wt % in water), and an aqueous solution of $Al(NO_3)_3$, respectively.

3. Results and Discussion

3.1. Structure Analysis of Dehydrated $AlPO_4$-SOD from Powder. The $AlPO_4$-**GIS** impurity in the dehydrated $AlPO_4$-**SOD** sample appeared during the dehydration process. It must be reminded here that $AlPO_4$-**GIS** can be synthesized under hydrothermal conditions at 170 °C in the presence of HF with DMF as cosolvent and template.[10] Under such acidic conditions, the dialkylformamide molecules are decomposed and dimethylammonium cations are occluded in the $AlPO_4$-**GIS** structure.[10] We propose, during the dehydration process at elevated temperature, small amounts of not well organized (amorphous) aluminum- and phosphorus-containing material react with some remaining DMF or dimethylammonium species to crystallize into $AlPO_4$-**GIS**.[10] The amorphous materiel was not readily detectable by X-ray powder diffraction nor by solid state NMR (probably due to overlapping). The F^- bridging groups present in $AlPO_4$-**GIS**[10] are replaced by OH^- species (no signal in the ^{19}F solid state NMR experiment).

After dehydration, there is still one template molecule per sodalite cage. However, one-third of the DMF molecules have moved in the direction of adjacent aluminum atoms, thereby rearranging the aluminum coordination spheres of 3 equiv of Al per sodalite cage that were coordinated by DMF molecules in the as-synthesized form (Figure 2). Of these three Al atoms, one is now coordinated by two DMF molecules, one by one DMF molecule, and one by zero DMF molecules, making these Al's 6-, 5-, and 4-coordinated. This explains the tripling of the unit cell volume and the presence of nine crystallographically different phosphorus and aluminum sites in the structure instead of three in the as-synthesized $AlPO_4$-**SOD**.[9] Seven Al atoms are in 4-fold coordination (Al1,2,3,6,7,8,9), one is 6-fold coordinated Al4 ($Al(DMF)_2O_4$, square bipyramid), and one is 5-fold coordinated Al5 ($Al(DMF)O_4$, trigonal bipyramid), while the nine independent phosphorus sites remain all tetrahedrally coordinated (see Figure 3). The distances and angles listed in Table 3 and Supporting Information Tables 2S and 3S are characteristic of tetrahedrally coordinated phosphorus and tetra-, penta-, and hexacoordinated aluminum atoms, respectively. Similar to as-synthesized $AlPO_4$-**SOD**,[9] the guest-framework

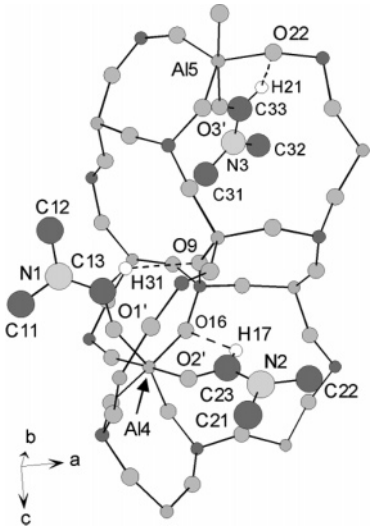

Figure 3. View of dehydrated $AlPO_4$-**SOD** where one DMF molecule is connected to Al5 and two others to Al4 to form a trigonal bipyramid and a square bipyramid, respectively.

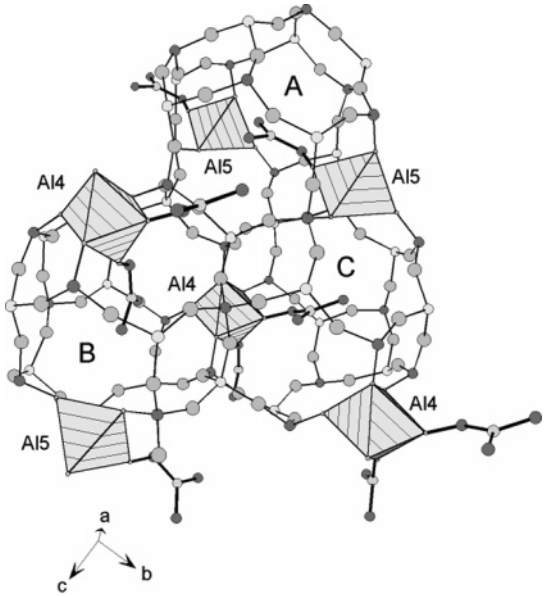

Figure 4. Drawing of the three kinds of sodalite cages (A, B, and C) present in dehydrated $AlPO_4$-**SOD**.

hydrogen-bonding scheme (Figure 3) involves the three carbonyl hydrogen atoms with O1′C−H31···O9 (2.39(3) Å), O2′C−H17···O16 (2.10(3) Å), and O3′C−H21···O22 (2.43(3) Å). However, as expected after dehydration, the protons of the methyl groups are slightly closer to the framework with a mean C−H···O distance of 2.86 Å compared to the mean C−H···O distance of 3 Å in the as-synthesized product.[9]

Three types of sodalite cages are generated by the dehydration. The cages A are shaped by 10 tetrahydrally coordinated aluminum atoms (Al1×2, Al2, Al3, Al6×2, Al7×2, Al8, Al9) and two 5-fold coordinated Al atoms (Al5), and cages B and C have nine tetrahydrally coordinated aluminum atoms ((Al2, Al3, Al6, Al7×2, Al8×2, Al9×2) and (Al1×2, Al2×2, Al3×2, Al6, Al8, Al9), respectively), one 5-fold coordinated aluminum atom Al5, and two 6-fold coordinated aluminum atoms Al4 (Figure 4).

3.2. Rehydration of the Dehydrated $AlPO_4$-SOD. *3.2.1. Powder X-ray Analysis.* Figure 5 represents the X-ray powder patterns of a dehydrated/rehydrated $AlPO_4$-**SOD** sample (48 h, 43 days, and 1 year). From these X-ray data, we can observe

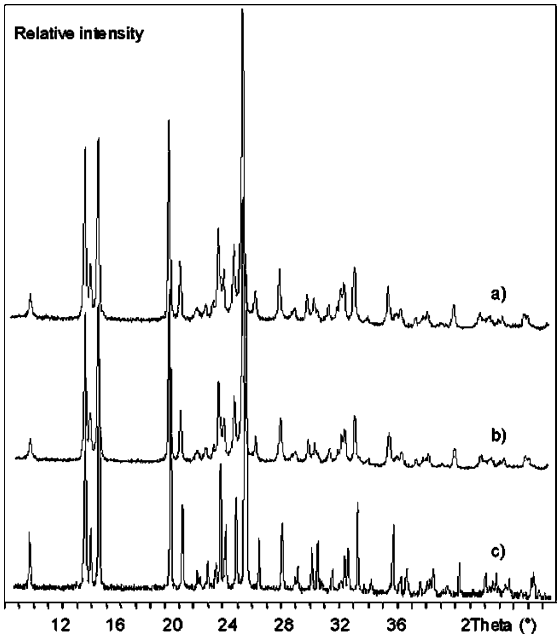

Figure 5. X-ray powder patterns of dehydrated/rehydrated $AlPO_4$-**SOD** after 48 h of rehydration (a), 43 days of rehydration (b), and 1 year of rehydration $AlPO_4$-**SOD** (c).

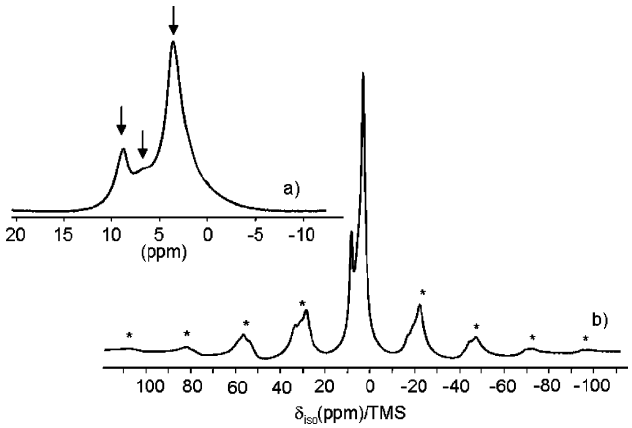

Figure 6. ^1H MAS NMR spectrum of dehydrated/rehydrated $AlPO_4$-**SOD** after 1 year at $\nu_R = 25$ kHz (a) and $\nu_R = 10$ kHz (b).

that, after a prolonged time of rehydration by exposure to a moisture atmosphere, the compound remains stable without the slightest partial decomposition into an amorphous material. In addition, the better resolution of the pattern (Figure 5c) observed after 1 year of rehydration compared to the one after 43 days suggests that the rehydration is very slow. It is worth noting that, after 1 year, the powder pattern of dehydrated/rehydrated $AlPO_4$-**SOD** is totally in accordance with the one of as-synthesized $AlPO_4$-**SOD**.[7,9]

3.2.2. Solid State NMR Study. ^1H MAS NMR. Figure 6 shows the ^1H MAS NMR spectrum of dehydrated/rehydrated material after 1 year, recorded at a spinning frequency of 25 kHz. Three signals (Figure 6a) could be distinguished at 8.8, 6.8, and 3.5 ppm of relative intensities 1:2:6, as is also observed for the as-synthesized $AlPO_4$-**SOD**.[9] The resonances at 8.8 and 3.5 ppm are assigned to protons belonging to the carbonyl and methyl groups of the dimethylformamide, respectively. The one at 6.8 ppm corresponds to protons from water molecules. The existence of spinning sidebands (Figure 6b) suggests a restricted mobility of the template and water molecules and consequently strong interaction between protons and aluminum atoms of the framework.

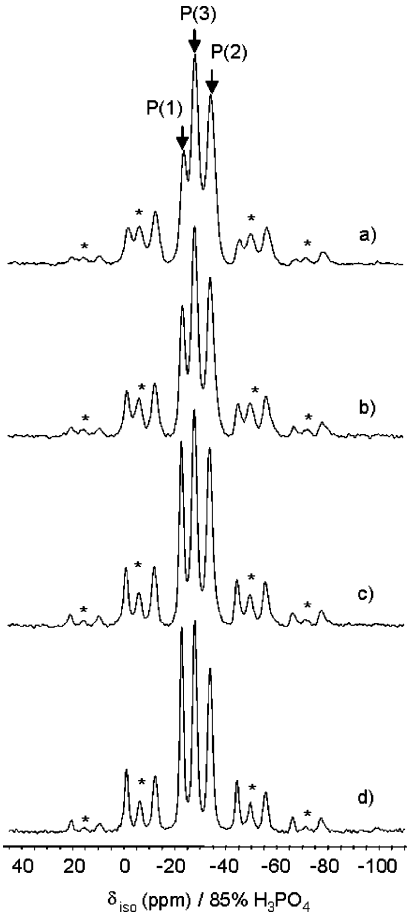

Figure 7. ^{31}P MAS NMR spectra of dehydrated/rehydrated $AlPO_4$-**SOD** at $\nu_R = 10$ kHz: 48 h of rehydration (a); 43 days of rehydration (b); 1 year of rehydration (c); as-synthesized $AlPO_4$-**SOD** (d).

^{31}P MAS NMR. ^{31}P MAS NMR spectra of the dehydrated/rehydrated materials present three distinct resonances independent of the rehydration time (Figure 7a−c). These spectra are identical to the spectrum of the as-synthesized $AlPO_4$-**SOD** (Figure 7d). Isotropic chemical shifts, tensor parameters, line widths, and relative intensities were estimated for each phosphorus crystallographic site, according to different hydration times (Supporting Information Table 4S). With increasing rehydration, all ^{31}P resonances sharpen and shift to higher frequencies, as is also observed for $AlPO_4$-11 or VPI-5.[5,15] After 1 year of rehydration, isotropic chemical shifts are similar to the as-synthesized $AlPO_4$-**SOD**. It is worth noting that the chemical shift tensor parameters η_{CS} and δ_{CS} (Supporting Information Table 4S) for the P(1) resonance vary strongly with the rehydration time, whereas this is not the case for the two other phosphorus resonances. Moreover, the relative intensity of the P(1) resonance slowly increased during rehydration. The P(1) crystallographic site seems to need more time to recover its initial state. These results show a slow and quasi-reversible rehydration process.

^{27}Al MAS NMR. The ^{27}Al MAS NMR spectra of dehydrated/rehydrated materials (48 h, 43 days, and 1 year) show two main signals (Figure 8a−c), one from 20 to 50 ppm and the other from −20 to −5 ppm, corresponding to tetra- and hexacoordinated aluminum atoms, respectively. However, after 48 h of rehydration, a small signal, between 0 and 13 ppm, is observed and assigned to pentacoordinated aluminums as in the fully dehydrated material. The presence of this Al^V resonance indicates that the hydration process is uncompleted. A 43 day rehydration allows the recovery of the ^{27}Al MAS NMR spectrum

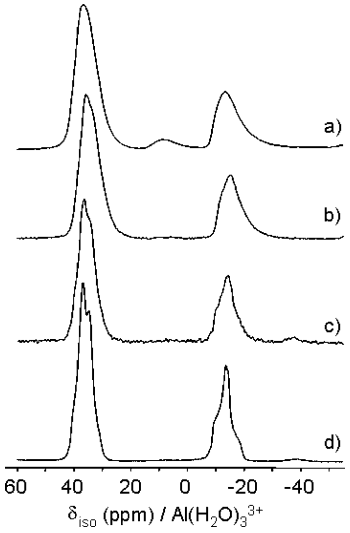

Figure 8. ^{27}Al MAS NMR spectra of dehydrated/rehydrated $AlPO_4$-**SOD** at $\nu_R = 10$ kHz: 48 h of rehydration (a); 43 days of rehydration (b); 1 year of rehydration (c); as-synthesized $AlPO_4$-**SOD** (d).

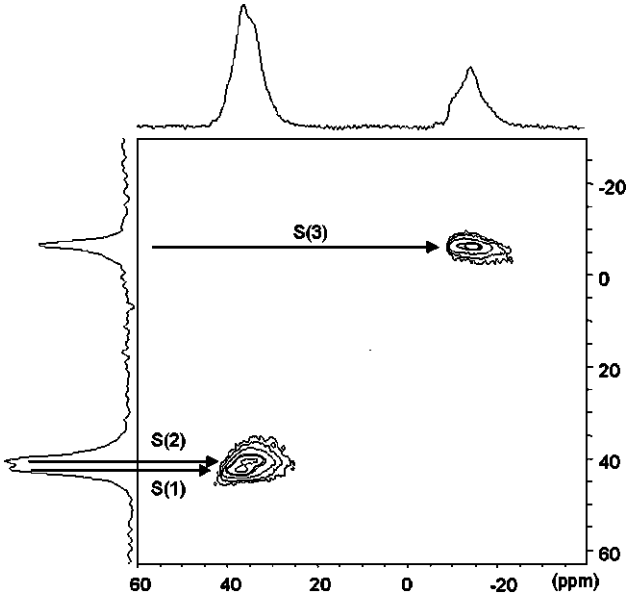

Figure 9. ^{27}Al sheared 3QMAS contour plot of 1 year rehydrated $AlPO_4$-**SOD** at $\nu_r = 15$ kHz. The arrows indicate the different aluminum sites. The ^{27}Al MAS NMR projection appears along the F2 dimension.

similar to the as-synthesized $AlPO_4$-**SOD** (Figure 8d), with an Al^{IV}/Al^{VI} intensity ratio of 0.66:0.33. A significant resolution improvement is observed for the Al^{IV} and Al^{VI} resonances in the 1 year rehydrated material (Figure 8c). Nevertheless, the ^{27}Al MAS NMR spectrum of the 1 year rehydrated material cannot be superimposed with the one of as-synthesized $AlPO_4$-**SOD**.

^{27}Al 3QMAS NMR. A ^{27}Al 3QMAS NMR experiment was performed in order to discriminate the number of Al^{IV} sites of the 1 year rehydrated sample. The result (Figure 9) exhibits two distinct tetrahedral aluminum resonances and one hexacoordinated aluminum resonance corresponding to the Al(3) site. Numerical simulations of the F2 slices (not shown) yield the quadrupolar coupling constant (C_Q) and the asymmetry parameter (η_Q) for each resonance (Table 4). The quadrupolar parameters are then used to simulate the ^{27}Al MAS NMR spectrum in order to determine the relative abundance of each site (Table 4). Chemical shifts and quadrupolar parameters are similar to those observed for the as-synthesized $AlPO_4$-**SOD**

TABLE 4: ^{27}Al Quadrupolar Interaction Parameters of Each Aluminum Site of 1 Year Rehydrated $AlPO_4$-SOD

	S(1)	S(2)	S(3)
δ_{iso} (ppm)	40.70	38.1	−9.9
C_Q (MHz) ± 0.1	2.4	2.5	2.6
$\eta_Q \pm 0.05$	0.7	0.7	0.8
%	35	35	30

(Supporting Information Figure 1S and Table 5S).[16] Consequently, the structural rearrangement of DMF molecules observed upon dehydration of the as-synthesized material seems to be reversible. This is in perfect agreement with the X-ray diffraction analysis which shows that, after 1 year of hydration of the dehydrated $AlPO_4$-**SOD**, the unit cell parameter *c* becomes similar to the one of the as-synthesized material.

4. Conclusion

The structure analysis of dehydrated $AlPO_4$-**SOD** was performed by molecular modeling and Rietveld analysis from synchrotron data. The hypothesis proposed earlier consisting of a tripling of the unit cell after dehydration of $AlPO_4$-**SOD** is fully confirmed by the present structure analysis. The dehydration/rehydration of $AlPO_4$-**SOD** is a reversible process but very slow. Indeed, as proved by X-ray and solid state NMR analysis, at least 1 year is necessary to completely rehydrate $AlPO_4$-**SOD**. This may be explained by the fact that $AlPO_4$-**SOD** has of course only six-ring pores.

Acknowledgment. We thank the staff of the Swiss-Norwegian Beamline at the ESRF in Grenoble for their help with the data collection for the dehydrated $AlPO_4$-**SOD** sample.

Supporting Information Available: Tables showing atomic, isotropic displacement, occupancy of the DMF molecules of dehydrated $AlPO_4$-**SOD**, selected interatomic distances, selected bond angles of dehydrated $AlPO_4$-**SOD**, isotropic chemical shifts, chemical shift tensor, and relative intensities for each phosphorus crystallographic site of dehydrated/rehydrated $AlPO_4$-**SOD**, ^{27}Al quadrupolar interaction parameters, line widths, and relative intensities of as-synthesized $AlPO_4$-**SOD**; figure showing a ^{27}Al 3QMAS contour plot of as-synthesized $AlPO_4$-**SOD**; and one cif file. This material is available free of charge via the Internet at http://pubs.acs.org.

References and Notes

(1) Wilson, S. T.; Lok, B. M.; Messina, C. A.; Cannan, T. R.; Flanigen, E. M. *J. Am. Chem. Soc.* **1982**, *104*, 1146−1147.

(2) Baerlocher, Ch.; Meier, W. M.; Olson, D. H. *Atlas of Zeolite Framework Types*, 5th ed.; Elsevier: Amsterdam, The Netherlands, 2001 (http://www.iza-structure.org/databases/).

(3) Tuel, A.; Calderelli, S.; Meden, A.; McCusker, L. B.; Baerlocher, Ch.; Ristic, A.; Rajic, N.; Mali, G.; Kaucic, V. *J. Phys. Chem. B* **2000**, *104*, 5697−5705.

(4) Barrie, P. J.; Smith, M. E.; Klinowski, J. *Chem. Phys. Lett.* **1991**, *180*, 6−12.

(5) Peeters, M. P. J.; de Haan, J. W.; van de Ven, L. J. M.; van Hooff, J. H. C. *J. Phys. Chem.* **1993**, *97*, 5363−5369.

(6) Peeters, M. P. J.; van de Ven, L. J. M.; de Haan, J. W.; van Hooff, J. H. C. *J. Phys. Chem.* **1993**, *97*, 8254−8260.

(7) Vidal, L.; Paillaud, J. L.; Gabelica, Z. *Microporous Mater.* **1998**, *24*, 189−197.

(8) Flanigen, E. M. In *New Developments in Zeolite Science and Technology*, Proceedings of the 7th International Zeolite Conference; Murakami, Y., Iijima, A., Ward, J. W., Eds.; Kodansha Ltd., Elsevier Science Publishers B. V.: Tokyo, Amsterdam, The Netherlands, 1986; pp 103−112.

(9) Roux, M.; Marichal, C.; Paillaud, J.-L.; Fernandez, C.; Baerlocher, Ch.; Chézeau, J. M. *J. Phys. Chem. B* **2001**, *105*, 9083−9092.
(10) Paillaud, J.-L.; Marler, B.; Kessler, H. *J. Chem. Soc., Chem. Commun.* **1996**, 1293−1294.
(11) *Cerius2 Modelling Environment*, release 4.2MS; Accelrys Inc.: San Diego, CA, 2002.
(12) (a) Larson, A. C.; Von Dreele, R. B. *General Structure Analysis System*, Los Alamos National Laboratory Report LAUR 86-748, 2000. (b) Toby, B. H. *J. Appl. Crystallogr.* **1994**, *34*, 210−213.
(13) Amoureux, J. P.; Fernandez, C.; Steuernagel, S. *J. Magn. Reson., Ser. A* **1996**, *123*, 116−118.
(14) Massiot, D.; Fayon, F.; Capron, M.; King, I.; Le Calvé, S.; Alonso, B.; Durand, J.-O.; Bujoli, B.; Gan, Z.; Hoatson, G. *Magn. Reson. Chem.* **2002**, *40*, 70−76.
(15) Maistrau, L.; Gabelica, Z.; Derouane, E. G. *Appl. Catal. A* **1992**, *81*, 67−80.
(16) Roux, M. Ph.D. Thesis, Université de Haute Alsace, Mulhouse, France, 2002.